Resonant hot-electron production in above-threshold ionization

P. Hansch, M. A. Walker, and L. D. Van Woerkom
Department of Physics, The Ohio State University, Columbus, Ohio 43210
(Received 18 November 1996)

We have observed surprising detailed structure in the photoelectron kinetic-energy spectrum of xenon under high-intensity short pulse conditions. We show that most of the photoelectrons with kinetic energies from 0–50 eV result from *resonant* processes at intensities up to 1.9×10^{14} W/cm^2. In particular, we find that the high-energy photoelectron structure in above-threshold ionization is actually composed of narrow individual peaks whose energy positions do not shift with intensity. The amplitudes of the structures change rapidly with intensity and turn on at different specific intensities. While those structures appear to be due to resonances, they cannot be attributed to *traditional* Rydberg transient resonances.
[S1050-2947(97)50404-5]

PACS number(s): 32.80.Rm, 32.80.Fb, 32.80.Wr

When an atom is exposed to intense radiation, the simultaneous absorption of many photons becomes probable. As the light intensity is increased the dominant ionization process occurs via multiphoton ionization (MPI) and subsequent above-threshold ionization (ATI) [1,2]. The latter process is characterized by the absorption of additional photons in the continuum. The corresponding photoelectron kinetic-energy spectra exhibit peaks that are separated by the photon energy.

Recent experiments by Walker *et al.* [3] and Paulus *et al.* [4] have revealed the production of hot electrons with kinetic energies as great as $11U_p$, where U_p is the ponderomotive energy [5]. The semiclassical explanation for these data involves the ''simpleman's theory'' or ''quasistatic model'' of ionization [6–8]. Both view strong field ionization as consisting of two independent steps: (i) an electron tunnels into the continuum at rest; (ii) the subsequent electron motion is governed by classical mechanics for a charged particle in an oscillating electric field. This idea has been very successful in describing the essential physics behind much of high harmonic generation; however, for ATI the model predicts a maximum kinetic energy of $2U_p$ [7] and must be modified to incloude backscattering [9,10] in order to create hot electrons.

The purpose of this paper is to present photoelectron kinetic-energy spectra showing prominent features at high kinetic energies that cannot be explained by simpleman-rescattering theory or *traditional* ATI via Rydberg-state resonances. Three different and unexplained effects have been seen. (i) We observe narrow dominant structures near 20 eV in the photoelectron kinetic energy spectra for xenon that indicate *resonant* ionization even at intensities as high as 1.9×10^{14} W/cm^2 and ponderomotive potentials above 10 eV. (ii) We find broader peaks near 35 eV comprised of at least two separate series of ATI peaks that do not shift with laser intensity. (iii) We measure large enhancements in the electron production for kinetic energies near 20 and 35 eV. The structures turn on within a very narrow intensity range between 1.2 and 1.9×10^{14} W/cm^2. Similar effects are also observed in argon and krypton in different kinetic-energy regions. Our measurements represent an enhanced level of resolution and signal-to-noise ratio for high-intensity photoelectron studies.

Narrow structures in the photoelectron kinetic-energy spectrum have been routinely seen for low kinetic energies and short pulse excitation. In 1987 the pioneering efforts of Freeman *et al.* [11] showed that in the limit of short laser pulses, where the photoelectron does not sample the spatial gradients of the laser focus, the resulting electron spectrum shows dramatic structure. This structure arises from the ac Stark shift of the atomic levels producing multiphoton resonances with harmonics of the laser field. Each ATI order breaks up into a series of narrow peaks corresponding to resonances with different Rydberg states. Each peak appears at a fixed kinetic energy corresponding to the precise intensity at which the atomic level shifts into resonance with the laser. A transient state with an initial energy E_i above the ground state produces photoelectrons with kinetic energies:

$$E = m\hbar\omega - IP - (n\hbar\omega - E_i), \tag{1}$$

where IP is the field-free ionization potential relative to the ground state, n indicates the harmonic at which the resonance occurs, and m $(>n)$ represents the total number of photons absorbed during the ionization. This expression is valid in the limit where the atomic levels shift ponderomotively and the small shift of the ground state is neglected.

The principal implication of the Stark-shifted resonance model is that photoelectron kinetic energies are fixed due to the multiphoton resonance occurring at a single laser intensity for each resonance. Thus, any electron-energy structure that does not shift with laser intensity must be due to some type of resonant process.

We have recorded high-resolution spectra over the intensity range near 10^{14} W/cm^2 in fine intensity steps. Our data show surprising structure within each ATI order for kinetic energies up to 50 eV. Furthermore, we see additional substructure near 20 eV, which does not appear in the 35–50-eV range. If these features resulted from nonresonant ionization, they would have to shift to lower kinetic energies as the peak

intensity increased. In contrast, our measurements show that no such shift occurs and that the hot electron features appear over a small intensity range, indicating a *resonant* ionization process. Traditional Rydberg transient resonances account unambiguously for the low-energy photoelectron structure found in experiments using linearly polarized light. For 800-nm light, Rydberg-state resonances yielding kinetic energies up to the $2U_p$ point can be clearly identified. Recently, the envelope of the electron signal beyond $2U_p$ has been attributed to inelastic backscattering. Very little attention, however, has been paid to the ATI structure in the region above $2U_p$ [9].

The spectra presented were obtained using a Positive Light, Inc. Ti:sapphire laser system operating at a 1-kHz repetition rate. The 120-fs, 800-nm output pulses have an energy of 700 μJ per pulse and are plane-polarized. Using a 25-cm focal length lens, intensities up to 1.9×10^{14} W/cm^2 can be achieved inside the interaction chamber. A traditional measure of the relative dominance of tunneling versus multiphoton effects is given by the Keldysh parameter $\gamma = \sqrt{IP/2U_p}$, where IP is the ionization potential and U_p is the ponderomotive potential. For xenon and the intensity range considered here we have $0.734 \leqslant \gamma \leqslant 0.897$, placing our experiment very slightly in the tunneling regime.

The shot-to-shot TEM_{00} mode intensity fluctuations are less than 5%. The kilohertz repetition rate allowed acquiring a minimum of 1×10^6 laser shots per spectrum. The high count rate yielded a statistical error on the order of 2% in the energy range of 20–60 eV, which indicates that the observed features are well above the noise. The photoelectron signal is recorded with a standard time-of-flight (TOF) spectrometer, and is detected with a pair of microchannel plates. The time resolution is 150 ps/bin, yielding an energy resolution of 0.4 meV for 1-eV electrons and 65 meV at 30 eV. The ultrahigh-vacuum spectrometer operates at a background pressure of 2×10^{-10} Torr. The acceptance angle of the detector is 3°. Spectra at different intensities have been recorded using intensity-selective scanning (ISS). This technique has been described elsewhere [12]. Briefly, a 500-μm pinhole is placed at the front of the TOF tube and only electrons traveling on the line of sight from the ionization volume to the detector are measured. This technique yields data from a one-dimensional radial intensity distribution, thereby reducing some of the problems associated with spatial averaging over the entire laser focal volume. By scanning a pinhole across the Gaussian ionization volume, specific peak intensities can be selected with high precision to produce an excellent signal-to-noise ratio.

Figure 1 shows a high-resolution photoelectron kinetic-energy spectrum of xenon from 2–50 eV. The spectrum consists of three basic regions: (i) 2–11 eV with well-defined Rydberg structure, (ii) 11–28 eV with narrow structure appearing as a function of intensity, and (iii) 28–50 eV with prominent ''bumps'' comprised of a number of ATI orders appearing as the intensity increases. It should be noted that the overall envelope of the electron signal does not monotonically decrease as predicted by various theoretical models. Although some calculations produce modulations in the spectrum for various kinetic energies [4,13], the experimentally observed signal enhancement between 15 and 50 eV is at least an order of magnitude larger than any current model predicts.

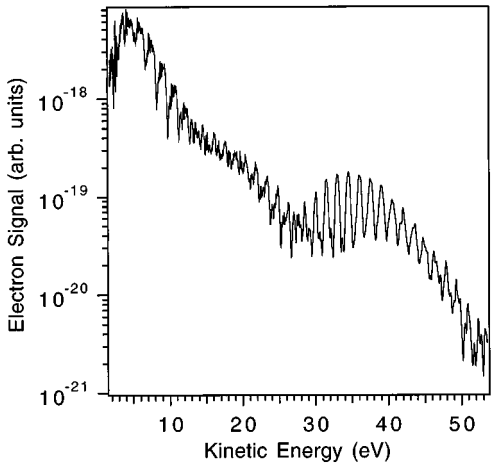

FIG. 1. Photoelectron spectrum of xenon with 800-nm, 120-fs pulses at 1.51×10^{14} W/cm^2.

The low kinetic-energy region consists of clear ac Stark-shifted Rydberg states, which can be identified up to 12 eV. The structure consists of the g states coming into nine-photon resonance with the laser field [14]. Although the basic photoionization processes producing these electrons is believed to be understood, there are in fact many subtleties that are unexplained. This fine structure continues at higher kinetic energies; however, it becomes extremely difficult to make assignments due to rapid variation in amplitude of the fine structure for different ATI orders.

Figure 2 shows the intermediate-energy region of the spectrum. The well-ordered Rydberg structure gives way to a series of narrow peaks that cannot be simply identified with

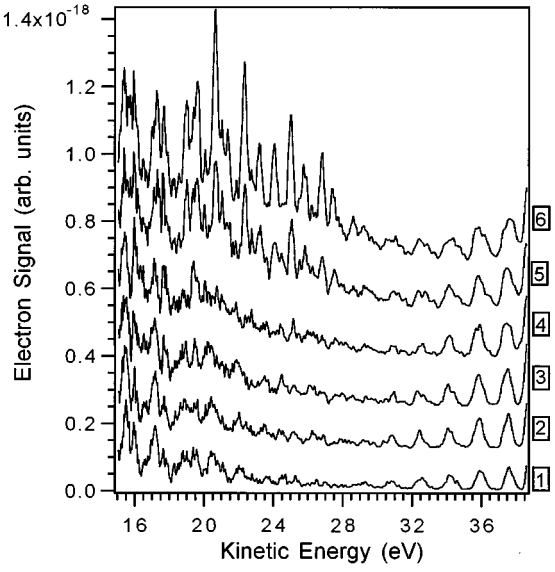

FIG. 2. Photoelectron spectra of xenon with 800-nm, 120-fs pulses at (1) 1.51, (2) 1.63, (3) 1.74, (4) 1.82, (5) 1.88, and (6) 1.90×10^{14} W/cm^2.

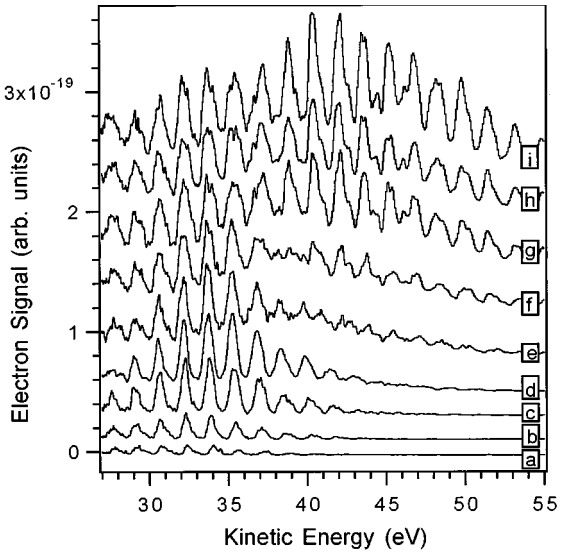

FIG. 3. Photoelectron spectra of xenon with 800-nm, 120-fs pulses at (a) 1.26, (b) 1.44, (c) 1.51, (d) 1.63, (e) 1.74, (f) 1.78, (g) 1.82, (h) 1.86, and (i) 1.88×10^{14} W/cm^2.

atomic levels. One of the difficulties in the hot electron portion of the spectrum is calibrating the energy scale from the measured time-of-flight data. Small variations in the time offset have dramatic effects in the higher kinetic energies. This not withstanding, we are unable to link the high-energy structures to the low-kinetic-energy f or g states or other Rydberg series. It is interesting to note the region between 20 and 30 eV. The photoelectron structures appears to vanish and reappear at higher energies. This is possibly a manifestation of the interference involving returning portions of the ionized wavepacket.

The high-energy portion of the kinetic energy spectrum is shown in Fig. 3. At intensities of $(1.26–1.74)\times10^{14}$ W/cm^2, the envelope of the spectra exhibits a bump, centered around 34 eV. Overall, there is a large modulation depth and the individual peaks are separated by the photon energy. Although we have sufficient resolution, no *fine* structure is detected within the ATI orders. The peaks in the range 28–40 eV increase in amplitude as the intensity rises, but they do not shift in energy. As they grow, shoulders develop on the higher-energy side. At intensities above 1.74×10^{14} W/cm^2 the peaks below 36 eV appear to saturate, while signal for the higher-energy electrons grows rapidly, indicating the enhancement of a second series of peaks. These peaks seem to rise out of the shoulders that developed in the first bump. While the peaks within each bump are exactly separated by the photon energy, there is an energy shift of about 0.5 eV between the two series. This supports the observation that at least two distinguishable series develop as the intensity increases. The intensity regime above 1.74×10^{14} W/cm^2 also corresponds to the appearance of the intermediate kinetic-energy peaks, as shown in Fig. 2. At the highest intensities, there are statistically significant small peaks between the dominant structure around 46 eV. This may be the onset of an additional series of peaks that is different from the first two.

No explanation exists for the observed structures. Clearly, a resonant process must be dominant since the individual peaks do not shift with laser intensity. Within the limits of our energy calibration, Rydberg states of the ion cannot be aligned with the measured structures. The saturation intensity for ionizing neutral xenon with 800-nm and 100-fs pulses is approximately 8×10^{13} W/cm^2 [15]. Although our measurements are above the saturation intensity, ion yield measurements made in our laboratory show that double ionization is not prominent [16]. Even though the number of double ions is small, it is still possible that portions of the photoelectron spectrum arise from double ionization but not by way of any *traditional* resonant mechanism.

Two key issues must be resolved. First, a process must be found that describes the resonant production of structure at high electron energies. Second, a mechanism for enhancing specific kinetic-energy regions must be found.

We propose a possible scenario for the production of narrow features at high energies involving multiply excited states. First, the issue of the fine structure could be dealt with through a combination of multiple excitations of the atom in the intense field. For example, an outer electron may be ''shelved'' in a Rydberg state and survive to higher intensities [17]. While the first electron remains far from the core, a remaining outer-shell electron can absorb a modest number of photons and be excited to the family of doubly excited states that exists in the heavier noble gases converging on the first double-ion limit. Subsequent autoionization will produce narrow features in the kinetic-energy range from 10–20 eV. Recall that this is the region marked by narrow features that cannot be assigned to traditional Rydberg resonances.

The enhancement between 30 and 50 eV could be due to a similar process. The difference is that an inner-shell excitation must be invoked in order to produce energies that high. One scenario involves the excitation of one of the $5s$ electrons in xenon. The $5s\rightarrow5p$ excitation requires about 11 photons at 800 nm. As mentioned earlier, the enhancement in this high-energy region is made up of at least two different peak series. Both features turn on very rapidly as soon as threshold intensities of 1.20 and 1.74×10^{14} W/cm^2 are reached for the bumps centered around 34 and 42 eV, respectively. In addition, the onset of very sharp strong features in the 20-eV region coincides with the growth of the 42-eV bump. Thus, the underlying physical process responsible for the high-energy bump could be linked to the intermediate-energy structures.

In conclusion, we have observed prominent structure in the hot electron production in high-intensity photoionization of xenon. The kinetic-energy regions near 20 and 35 eV show an enhancement in electron production. It is clear that a resonant process must be involved due to the lack of kinetic-energy shifts with laser intensity. Finally, we propose that the mechanism involves coupling to other valence or inner-shell electrons. Much work remains to be done on both the experimental and theoretical sides in order to explain these phenomena.

The authors would like to acknowledge fruitful discussions with Professor Phil Bucksbaum and Marcus Hertlein. This material is based upon work supported in part by the U. S. Army Research Office under Grant No. DAAH04-95-1-0418.

[1] P. Agostini, F. Fabre, G. Mainfray, G. Petite, and N. K. Rahman, Phys. Rev. Lett. **42**, 1127 (1979).
[2] P. Kruit, J. Kimman, and M. J. Van der Wiel, J. Phys. B **14**, L597 (1981).
[3] B. Walker *et al.*, Phys. Rev. Lett. **73**, 1227 (1994).
[4] G. G. Paulus, W. Nicklich, H. Xu, P. Lambropoulos, and H. Walther, Phys. Rev. Lett. **72**, 2851 (1994).
[5] The ponderomotive energy U_p is defined in atomic units as $I/4\omega^2$, where I and ω are the laser intensity and frequency, respectively. For 800-nm photons, $U_p=5.98$ eV at 10^{14} W/cm^2.
[6] *Studies in Modern Optics No. 8, Multiphoton Processes*, edited by H. B. van Linden van den Heuvell and H. G. Muller (Cambridge University Press, Cambridge, 1988).
[7] T. F. Gallagher, Phys. Rev. Lett. **61**, 2304 (1988).
[8] P. B. Corkum, N. H. Burnett, and F. Brunel, Phys. Rev. Lett. **62**, 1259 (1989).
[9] G. G. Paulus, W. Becker, W. Nicklich, and H. Walther, J. Phys. B **27**, L703 (1994).
[10] W. Becker, A. Lohr, and M. Kleber, J. Phys. B **27**, L325 (1994).
[11] R. R. Freeman *et al.*, Phys. Rev. Lett. **59**, 1092 (1987).
[12] P. Hansch and L. D. Van Woerkom, Opt. Lett. **21**, 1286 (1996).
[13] M. Lewenstein, K. C. Kulander, K. J. Schafer, and P. H. Bucksbaum, Phys. Rev. A **51**, 1495 (1995).
[14] P. Hansch, M. A. Walker, and L. D. Van Woerkom (unpublished).
[15] L. DiMauro (private communication).
[16] P. Hansch, M. A. Walker, and L. D. Van Woerkom, Phys. Rev. A **54**, R2559 (1996).
[17] R. R. Jones, D. W. Schumacher, and P. H. Bucksbaum, Phys. Rev. A **47**, R49 (1993).